Ultra broadband-flattened dispersion photonic crystal fiber for supercontinuum generation

Liang Fang (方 亮), Jianlin Zhao (赵建林)*, and Xuetao Gan (甘雪涛)

Shaanxi Key Laboratory of Optical Information Technology, School of Science, Northwestern Polytechnical University, Key Laboratory of Space Applied Physics and Chemistry, Ministry of Education, Xi'an 710072, China

**E-mail: jlzhao@nwpu.edu.cn*

Received March 26, 2010

We propose an improved design of photonic crystal fiber (PCF) with ultra broadband-flattened dispersion and ultra-low confinement loss in the telecommunication window. The design is considerably suitable for the generation of wideband supercontinuum spectrum. Numerical results reveal that the proposed PCF structure possesses a low dispersion of 0±1.5 ps/(nm·km) in the wavelengths ranging from 1.134 to 1.805 μm (approximately 700-nm bandwidth) with a confinement loss of less than 10^{-8} dB/km. In addition, a nonlinear coefficient greater than 11.47 $(\mathrm{W\cdot km})^{-1}$and a dispersion slope of as low as −0.005694 ps/($\mathrm{nm^2\cdot km}$) are obtained at 1.55-μm wavelength. Moreover, a symmetric flat supercontinuum spectrum with a 10-dB bandwidth of 190 nm is achieved in a 3-m-long fiber, verifying the excellent optical features of the innovative PCF.

OCIS codes: 060.2280, 060.2400, 060.4370.
doi: 10.3788/COL20100811.1028.

Photonic crystal fibers (PCFs)[1], which are characterized by artificially periodic cladding consisting of micrometer-sized air holes running along the length, have attracted increasing attention in the past decade. In PCFs, the additional design parameters of size, number, and position of air holes provide considerable flexibility in the design of guiding properties. Moreover, the high index difference between the silica core and the holey cladding can confine light more tightly than do conventional fibers. As a result, PCFs have been reported to possess attractive optical characteristics, such as endless single-mode operation[2], controllable nonlinearity[3], high birefringence[4], and ultra-flattened chromatic dispersion with low confinement loss[5], etc. These attributes enable different potential applications. Controlling chromatic dispersion, especially in the telecommunication window, is a key problem in the application of PCFs, influencing such areas as the design of practical optical communication systems[6], wavelength conversions[7], and nonlinear systems[8]. With the recent development of PCFs, supercontinuum (SC) generation has been a focus of intense research because the wideband light source has already been applied in various fields such as optical coherence tomography, all-optical signal processing, and frequency metrology. Therefore, PCFs with ultra-flattened dispersion profiles—favored candidates in SC generation—have been extensively investigated not only in their initial appearance[9,10] but also in current designs[3,5,11−13]. Moreover, other important characteristics of PCFs, namely, low confinement loss and high nonlinearity, are essential to efficient and symmetric SC generation.

To date, several designs of PCFs have been reported to present remarkable dispersions and leakage properties. Flattened dispersion of conventional PCFs with identical cladding air holes has been experimentally realized by modifying hole size. However, a large number of ring layers are needed to reduce the confinement losses to a satisfactorily applicable level, possibly adding complexity to the fabrication process[10]. Controlling the dispersion slope in a wide wavelength range is also difficult[9]. Enlarging the air holes ring by ring along the fiber radius has been theoretically demonstrated to be able to solve the previously mentioned problems[14]; however, this imposes significant fabrication challenges. In addition, many other special designs, such as the GeO_2 doping concentration of the core[11]and filling the air holes with selective liquids[15], have been presented, but can thus far be studied conveniently only in theory. Recently, dual concentric core PCFs have been extensively recommended for their modest number of parameters and preferred optical properties[3,5,12,16,17]. As a part of ongoing efforts to design simple PCFs with flattened dispersion and low confinement loss, we propose an improved PCF structure with a modest number of parameters including three air hole diameters, eight rings, and a single air hole pitch.

The proposed PCF structure combines the advantages of the PCFs mentioned in Refs. [9] and [14]; its schematic cross section is depicted in Fig. 1. To simplify the fabrication technique, the air holes have only three different diameters, i.e., the inner two rings, middle two rings, and outer four rings have their own diameters denoted by d_1, d_2, and d, respectively. To conveniently control the dispersion and confinement loss, the diameters need to satisfy the condition $d_1 < d_2 < d$. The air hole pitch labeled Λ has only one value in the PCF. The above structure reflects a design idea that adjusts the chromatic dispersion of the PCF by increasing the diameters of the air holes every two rings in the inner six rings. Here, it should be noted that, the air holes in the seventh and eighth rings are used to diminish the confinement loss, whose diameter has little influence on the dispersion profile[12] and is chosen to be the same as that in the fifth and sixth rings to facilitate the fabrication process. Notice that although the

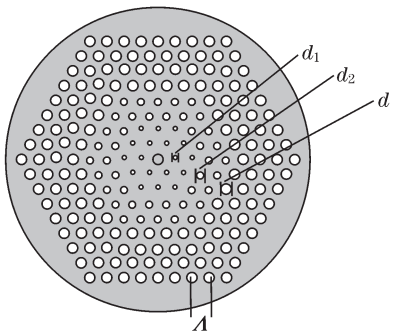

Fig. 1. Geometry of the proposed eight-ringed PCF with a single pitch and three types of air hole diameters.

configuration of the inner four rings of our PCF appears to be similar with that of the PCF structure referred to in Refs. [16] and [17], the design idea in our proposed PCF structure has not been presented in these two reports. This improved PCF structure is expected to provide ultra broadband-flattened chromatic dispersion characteristics with extremely low confinement loss, high nonlinearity, and low dispersion slope in the telecommunication window. This structure is extremely suitable for the generation of wideband SCs.

The vector wave equation describing the electric field vector $\mathbf{E}(x,y,z)$ propagating along the z-axis in PCFs can be deduced from Maxwell's equations as

$$\nabla \times \left([s]^{-1} \nabla \times \mathbf{E} \right) - k_0^2 n^2 [s] \mathbf{E} = 0, \tag{1}$$

where $k_0 = 2\pi/\lambda$ is the wave number and λ is the wavelength, n is the refractive index, $[s]$ is the anisotropic perfectly matched boundary layer matrix chosen to enclose the computational domain without affecting the numerical simulation, and $[s]^{-1}$ is the inverse matrix of $[s]$. The solution of Eq. (1) is identified in the form $\mathbf{E}(x,y,z) = \boldsymbol{\psi}(x,y,z)\exp(-\mathrm{i}\beta z)$ by employing the finite-difference frequency-domain (FDFD) method, where β is the complex propagation constant, whose imaginary and real components are the attenuation and phase constants, respectively. The complex propagation constant has a relationship of $n_{\mathrm{eff}} = \beta/k_0$ with effective refractive index n_{eff}. Hence, the confinement loss L_{c} in units of dB/m, determined by the attenuation constant, i.e., $\mathrm{Im}[\beta]$ is[18]

$$L_{\mathrm{c}} = \frac{20}{\ln 10} \times \mathrm{Im}[\beta] = 8.686 k_0 \times \mathrm{Im}[n_{\mathrm{eff}}]. \tag{2}$$

The relationship between waveguide chromatic dispersion $D_{\mathrm{w}}(\lambda)$ in ps/(nm·km) and the real component of effective refractive index $\mathrm{Re}[n_{\mathrm{eff}}]$ is governed by

$$D_{\mathrm{w}}(\lambda) = -\frac{\lambda}{c} \frac{\mathrm{d}^2 \{\mathrm{Re}[n_{\mathrm{eff}}]\}}{\mathrm{d}\lambda^2}, \tag{3}$$

where c is the light speed in vacuum. Moreover, based on the solution of $\mathbf{E}(x,y,z)$, the effective area A_{eff} and nonlinear coefficient γ of the PCFs can be described by

$$A_{\mathrm{eff}} = \frac{\left(\int_{-\infty}^{\infty} \int_{-\infty}^{\infty} |\mathbf{E}|^2 \, \mathrm{d}x \mathrm{d}y \right)^2}{\int_{-\infty}^{\infty} \int_{-\infty}^{\infty} |\mathbf{E}|^4 \, \mathrm{d}x \mathrm{d}y}, \tag{4}$$

$$\gamma = 2\pi \frac{n_2}{\lambda A_{\mathrm{eff}}}, \tag{5}$$

respectively, where $n_2 = 3\times10^{-20}$ m^2/W is the nonlinear refractive index. The total dispersion, which we focus on in this letter, can be obtained as the sum of the waveguide dispersion and the material dispersion:

$$D(\lambda) \approx D_{\mathrm{w}}(\lambda) + D_{\mathrm{m}}(\lambda), \tag{6}$$

where material dispersion $D_{\mathrm{m}}(\lambda)$ can be acquired directly from the three-term Sellmeier formula, and waveguide dispersion $D_{\mathrm{w}}(\lambda)$ is determined by Eq. (3).

In PCFs, the air holes in the outer rings have little influence on dispersion tailoring[12], and the periodicity in the cladding region is not essential to confining the guiding light within the high-index core region[19]. Hence, we mainly focus on the effects of d_1, d_2, and Λ on the dispersion properties, in which we can accordingly modulate the dispersion profiles to be ultra-flattened. First, we discuss the changes of dispersion profiles by varying Λ in two PCFs with $d_1 = 0.8$ μm, $d_2 = 1.28$ μm, and $d = 1.44$ μm, as well as $d_1 = 0.64$ μm, $d_2 = 1.28$ μm, and $d = 1.44$ μm, as shown in Figs. 2(a) and (b), respectively. The results in the two cases reveal that as the value of pitch Λ increases, the dispersions visibly descend in the short-wavelength range, and the curves ascend in the long-wavelength range. In other words, the slopes of the dispersion curves decrease to a small value before increasing. Therefore, an optimal Λ is expected to be chosen to achieve dispersion slope tuning. In Fig. 2(b), we find that the dispersion profile of the PCF with $d_1 = 0.64$ μm, $d_2 = 1.28$ μm, $d = 1.44$ μm, and $\Lambda = 1.8$ μm has two inflexions around the 1.55-μm wavelength, which are very close to the zero dispersion value. Thus, the PCF with wideband nearly-zero flattened dispersion can be realized on the basis of this preliminary design.

Next, we change diameter d_1 of the air holes in the inner two rings and study the influence of this parameter on the dispersion, illustrated in Fig. 3(a). The dispersion curves reveal that with the increment of d_1, the maxima of the four curves in the short-wavelength range ascend around the 1.2-μm wavelength; however, in the long-wavelength range, their tails drop down and have a crossing point around the 1.6-μm wavelength. These all enable the possibility of designing a flattened dispersion PCF around the telecommunication window. Moreover, dispersion curves clearly change drastically even with tiny changes of d_1; thus, the diameter of the inner two rings plays an important role in the dispersion tailoring. Based on this conclusion, we adjust the PCF to present a

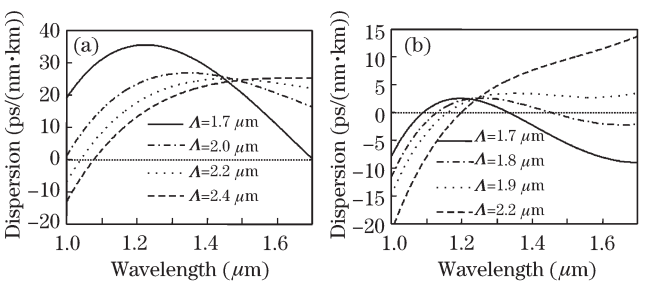

Fig. 2. Dispersions of PCFs by changing pitch Λ and retaining (a) $d_1 = 0.8$ μm, $d_2 = 1.28$ μm, $d = 1.44$ μm; (b) $d_1 = 0.64$ μm, $d_2 = 1.28$ μm, $d = 1.44$ μm.

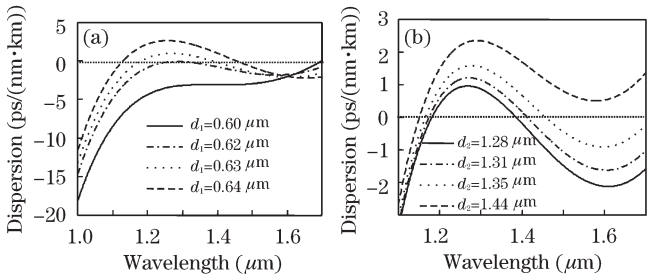

Fig. 3. Dispersions of PCFs with (a) $\Lambda = 1.8$ μm, $d_2 = 1.28$ μm, $d = 1.44$ μm by changing d_1; with (b) $\Lambda = 1.8$ μm, $d_1 = 0.63$ μm, $d = 1.44$ μm by changing d_2.

symmetric dispersion profile around the zero dispersion value, as the curve corresponding to $\Lambda = 1.8$ μm, $d_1 = 0.63$ μm, $d_2 = 1.28$ μm, and $d = 1.44$ μm shown in Fig. 3(a). Then, the diameter d_2 of the air holes in the middle two rings is varied and other parameters are retained: $\Lambda = 1.8$ μm, $d_1 = 0.63$ μm, and $d = 1.44$ μm. The dispersion behaviors of PCFs caused by tuning d_2 are shown in Fig. 3(b). Interestingly, although the dispersion curves have less variation than those in Fig. 3(a), the shift is larger in the long-wavelength range than in the short-one. This effect is opposite to that of d_1, which has significantly larger dispersion modification at a shorter wavelength than at a longer wavelength. Hence, our proposed PCF structure can possibly obtain a flattened dispersion over an ultra-wide wavelength range by finely adjusting d_1 and d_2 simultaneously. The PCF with $\Lambda = 1.8$ μm, $d_1 = 0.63$ μm, $d = 1.44$ μm, and $d_2 = 1.31$ μm in Fig. 3(b) indicates that its dispersion profile exhibits a nearly-zero flattened dispersion around 1.55 μm, and we choose this to proceed to the next stage of refinement.

Based on the analysis above, further calculations show that an optimal PCF structure can be obtained with

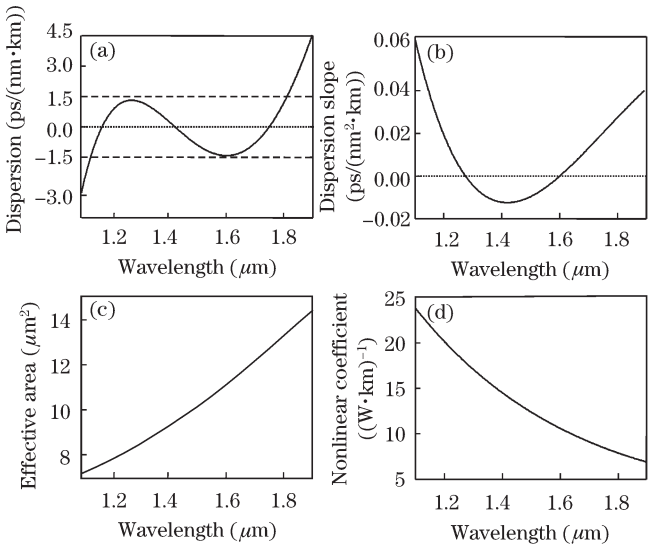

Fig. 4. (a) Dispersion, (b) dispersion slope, (c) effective area, and (d) nonlinear coefficient of the proposed PCF with $\Lambda = 1.8$ μm, $d_1 = 0.63$ μm, $d_2 = 1.32$ μm, $d = 1.44$ μm as a function of wavelength.

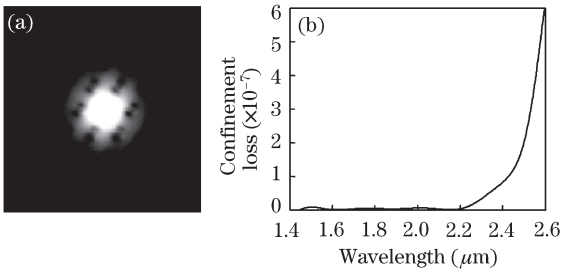

Fig. 5. (a) Mode field pattern of the fundamental mode at 1.5 μm and (b) confinement loss of the proposed PCF.

parameters $\Lambda = 1.8$ μm, $d_1 = 0.63$ μm, $d_2 = 1.32$ μm, and $d = 1.44$ μm; this structure's dispersion profile and dispersion slope are presented in Figs. 4(a) and (b), respectively. A symmetric ultra-flattened dispersion profile is achieved between ±1.5 ps/(nm·km) within a wide wavelength range of 1.134 − 1.805 μm. The dispersion slope fluctuates from −0.01261 to 0.04579 ps/(nm^2·km), and is −0.005694 ps/(nm^2·km) at 1.55 μm. Figures 4(c) and (d) show the effective mode area and nonlinear coefficient of the proposed PCF as a function of wavelength. We find that at the wavelength of 1.55 μm, the effective mode area is 10.6 μm^2, and the corresponding nonlinear coefficient is greater than 11.47 (W·km)$^{-1}$. This value is less than that mentioned in Refs. [3] and [19] because of the relatively larger air hole pitch of our optimal structure. However, this broad bridge between the air holes has little effect on the ability to collect light into the core of the PCF. The mode field intensity distribution of the optimal structure at 1.55-μm wavelength shown in Fig. 5(a) illustrates that the field has been well confined in the core because no obvious light leakage into the cladding region beyond the first ring is observed. The analysis in Fig. 5(b) further verifies this, showing that the confinement loss is in the order of 10^{-8} dB/km around 1.55 μm—significantly lower than that reported in other recent PCF designs[3,5,12]. This value increases when the ring number decreases and corresponds to the seven-ringed structure, to 10^{-5} dB/km—a value close to that obtained in Refs. [3] and [5]. Furthermore, without the outer two cladding rings, the six-ringed PCF exhibits a confinement loss of 10^{-2} dB/km, demonstrating that our design idea can provide a PCF structure with low confinement loss. The ultra-low confinement loss of our eight-ringed PCF structure can provide crucial advantages in numerous applications.

To confirm the optical characteristics of our proposed PCF, SC generation in the PCF is numerically investigated by exploiting the nonlinear Schrödinger equation

$$\frac{\partial A}{\partial z} + \sum_{n=2} \beta_n \frac{\mathrm{i}^{n-1}}{n!} \frac{\partial^n}{\partial T^n} A = \mathrm{i}\gamma \left[|A|^2 A + \frac{\mathrm{i}}{\omega_0} \frac{\partial}{\partial T} \left(|A|^2 A \right) - T_\mathrm{R} A \frac{\partial |A|^2}{\partial T} \right], \quad (7)$$

where A is the complex amplitude of the optical wave field, β_n is the nth order of the Taylor series expansion

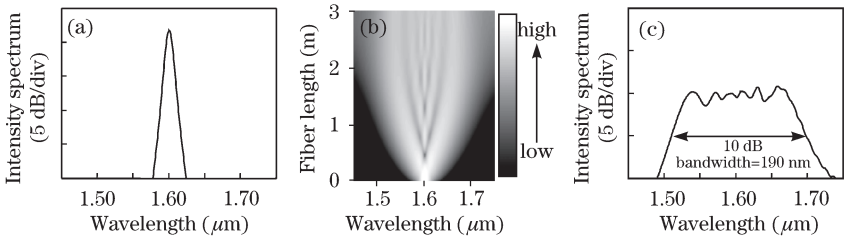

Fig. 6. SC generation in the proposed PCF. (a) Input spectrum, (b) evolution of spectrum, and (c) output spectrum.

of the propagation constant around the carrier frequency (here we choose n from 1 to 6), γ is the nonlinear coefficient determined by Eq. (5), and $T_{\rm R}$ is the Raman scattering parameter. This equation is solved using split-step Fourier method[20,21], in which the propagation distance of the optical field is divided into many unit segments, and the dispersive and nonlinear effects are simulated to act independently over each unit segment.

We consider the propagation of a sech^2 waveform with full-width at half-maximum $T_{\rm FWHM} = 260$ fs, peak power $P_0 = 1000$ W, and center wavelength $\lambda_{\rm P} = 1.6$ μm through the optimal PCF. Figure 6 shows the generation process of the SC in the 3-m-long fiber, where Figs. 6(a), (b), and (c) represent the input spectrum, evolution of the spectrum, and the output spectrum, respectively. We can observe that because of the ultra-flattened dispersion of the proposed PCF, the input pulse undergoes rapid broadening at its initial propagation; then, a relatively symmetric flat SC spectrum with 10-dB bandwidth of 190 nm is achieved at 3-m length. In comparison with the SC generation in Ref. [19], we find that although the proposed PCF possesses lower nonlinearity, the band of the generated SC is significantly wider due to the ultra-broad flattened dispersion and ultra-low confinement loss. In addition, the length of PCF is enormously shortened.

In conclusion, we have proposed an improved PCF structure, with air holes that increase every two rings—an approach that can be used to control and design PCFs with nearly-zero flattened dispersion in an ultra-wide wavelength range in the telecommunication window and ultra-low confinement loss. Our numerical simulations demonstrate that the PCF may be adjusted to achieve a flattened dispersion of 0 ± 1.5 ps/(km·nm) over a wavelength between 1.134 and 1.805 μm with a confinement loss of less than 10^{-8} dB/km. The proposed PCF, intended for application in the telecommunication system, exhibits a dispersion slope of as low as -0.005694 ps/(nm^2·km) and a nonlinear coefficient greater than 11.47 (W·km)$^{-1}$ at the wavelength of 1.55 μm. Remarkably, this wideband-flattened dispersion profile can support an effective SC generation with a 10-dB bandwidth of 190 nm despite a short fiber length of 3 m. Compared with the previously reported PCFs, the design procedure for the proposed PCF may be less complicated with relatively fewer parameters requiring optimization. This improved PCF structure is expected to have a considerable effect on numerous engineering applications, such as dispersion compensation, ultra-short soliton pulse transmission, and wavelength-division multiplexing transmission.

This work was supported by the Northwestern Polytechnical University Foundation for Fundamental Research and Open Research Fund of the State Key Laboratory of Transient Optics and Photonics, Chinese Academy of Sciences.

References

1. J. Broeng, D. Mogilevstev, S. E. Barkou, and A. Bjarklev, Opt. Fiber Technol. **5,** 305 (1999).
2. T. A. Birks, J. C. Knight, and P. St. J. Russell, Opt. Lett. **22,** 961 (1997).
3. F. Begum, Y. Namihira, S. M. A. Razzak, S. Kaijage, N. H. Hai, T. Kinjo, K. Miyagi, and N. Zou, Opt. Commun. **282,** 1416 (2009).
4. S. Kim, C. Kee, and C. G. Lee, Opt. Express **17,** 7952 (2009).
5. Y. M. Wang, X. Zhang, X. M. Ren, L. Zheng, X. L. Liu, and Y. Q. Huang, Appl. Opt. **49,** 292 (2010).
6. M. D. Nielsen, C. Jacobsen, N. A. Mortensen, J. R. Folkenberg, and H. R. Simonsen, Opt. Express **12,** 1372 (2004).
7. Q. Wang, B. Yang, L. Zhang, H. Zhang, and L. He, Chin. Opt. Lett. **5,** 538 (2007).
8. V. Finazzi, T. M. Monro, and D. J. Richardson, J. Opt. Soc. Am. B **20,** 1427 (2003).
9. A. Ferrando, E. Silvestre, P. Andres, J. J. Miret, and M. V. Andres, Opt. Express **9,** 687 (2001).
10. W. H. Reeves, J. C. Knight, P. St. J. Russell, and P. J. Roberts, Opt. Express **10,** 609 (2002).
11. S. Lou, H. Fang, H. Li, T. Guo, L. Yao, L. Wang, W. Chen, and S. Jian, Chin. Opt. Lett. **6,** 821 (2008).
12. W. Wang, L. T. Hou, J. J. Song, and G. Y. Zhou, Chin. Phys. Lett. **26,** 054204 (2009).
13. M. Wu, H. Liu, and D. Huang, Acta Opt. Sin. (in Chinese) **28,** 539 (2008).
14. K. Saitoh, M. Koshiba, T. Hasegawa, and E. Sasaoka, Opt. Express **11,** 843 (2003).
15. K. M. Gundu, M. Kolesik, J. V. Moloney, and K. S. Lee, Opt. Express **14,** 6870 (2006).
16. T. Wu and C. Chao, IEEE Photon. Technol. Lett. **17,** 67 (2005).
17. T. Wu and C. Chao, J. Lightwave Technol. **23,** 2055 (2005).
18. K. Saitoh and M. Koshiba, Opt. Express **11,** 3100 (2003).
19. K. Saitoh and M. Koshiba, Opt. Express **12,** 2027 (2004).
20. J. W. Cooley and J. W. Tukey, Math. Comput. **19,** 297 (1965).
21. X. Cui, J. Zhao, D. Yang, P. Li, W. Zhao, and Y. Wang, Chinese J. Lasers (in Chinese) **36,** 2046 (2009).